agronomy

Article

Determining Irrigation Volumes for Enhancing Profit and N Uptake Efficiency of Potato Using WASH_2D Model

Shuoshuo Liang, Hassan M. Abd El Baki, Ping An and Haruyuki Fujimaki *

Arid Land Research Center, Tottori University, Tottori 680-0001, Japan
* Correspondence: fujimaki@tottori-u.ac.jp

Abstract: Soaring food prices and the intensified scarcity of water resources put a new emphasis on efficient use of water in irrigation. Numerical models for water flow and crop growth can be used to predict crop water stress and make decisions on irrigation management. To this end, a new irrigation scheme was presented to determine the optimum irrigation depths using WASH_2D, a numerical model of water flow and solute transport in soils and crop growth. By using freely available quantitative weather forecasts and volumetric water price as input data to predict soil water flow and give the recommendation of irrigation depths which maximizes net income during each irrigation interval. Field experiments using potato were conducted for two-seasons in a sandy soil in Japan under three irrigation methods, i.e., using the simulation model named treatment "S" (to distinguish, named S1 in first season and S2 in second season), automatic irrigation method using soil moisture sensors named treatment "A", and refilling irrigation management supplying 100% consumed water named treatment "R". To compare S with other two treatments, S1 and A was conducted in the first season, then S2 and R was conducted in the second season. Results showed that S1 improved potato yield by 19%, and reduced water by 28%, resulting in an increased net income by 19% compared with A in the first season. There was no significant difference when compared with R in the second season, which was mainly due to the frequent rainfall during second growing season. In addition, S improved the nitrogen uptake efficiency (NU_PE) by 39% and 11% compared with A and R, respectively. The simulated values of water content were in fair agreement with those measured in the root zone. In short, simulated irrigation method was effective in improving yield, saving water and increasing NU_PE of potato compared with automatic and refilling irrigation methods in sandy field.

Keywords: net income; sandy soil; nitrogen uptake efficiency; transpiration; dryland

Citation: Liang, S.; Abd El Baki, H.M.; An, P.; Fujimaki, H. Determining Irrigation Volumes for Enhancing Profit and N Uptake Efficiency of Potato Using WASH_2D Model. *Agronomy* **2022**, *12*, 2372. https://doi.org/10.3390/agronomy12102372

Academic Editors: Antonella Lavini and Mohamed Houssemeddine Sellami

Received: 9 September 2022
Accepted: 27 September 2022
Published: 30 September 2022

1. Introduction

Irrigated agriculture has been the primary user of water in arid and semi-arid zones, which occupies over 70–80% of the total, especially in the water scarce area [1]. Continued population growth, limited water supply, and climate change require measures to conserve water in agriculture [2]. At present and more so in the future, irrigation in a conservation and sustainable way will be the norm rather than the exception. Nevertheless, many farmers still irrigate in the way of unsustainability [3,4]. The development of more precise and efficient irrigation management is still required. Many studies have focused on reducing the amount of irrigation by supplying water below the needs of crop, termed regulated deficit irrigation (RDI), with the purpose of improving crop water productivity (CWP) [5]. However, it is net income rather than CWP that farmers expected to maximize from their agricultural activities, and the maximization of net income should be a prerequisite for sustainable farming [6]. New irrigation schemes aimed at improving net income of farmers should be proposed.

Irrigation events are usually carried out based on soil water status, in which soil moisture is measured to determine the irrigation need or estimated using soil water balance equation. Then the irrigation quota is determined according to the water consumption during the irrigation interval, applying water to meet the crop water requirement (100% ET), or less than crop requirement (lower than 100% ET) [7–9]. In addition, most of studies have provided solutions for long-term decision making of water allocation to different growth stages of crop using meteorological data of previous years. But interannual variability in climate varies too widely to give accurate irrigation depth at each time [10]. Therefore, weather forecast (WF) data, as a freely and easily accessible online information, is gradually being incorporated into irrigation decisions, and has been proved that it can save irrigation water if properly utilized [11]. Brown [12] found that incorporating 2-day weather forecast could reduce water use by 1.5–2.3%, and 3.9–4.6% reduction in water use when 5-day forecast information was incorporated. Lorite et al. [13] compared reference evapotranspiration (ET_0) determined on one day and weekly weather forecast with measured data, and found the performance of weather forecast is acceptable. Muller et al. [14] examined the economic output of incorporating weather forecast into irrigation decisions, predicting that 5% additional profit would be possible when weather forecast is incorporated into the decisions. Anupoju V et al. [15] modified the SWAP model by considering different weather forecast horizons (1, 3, and 5 days), and found conventional irrigation (without weather forecast) resulted in higher water use, percolation losses and lower yield. The successful implementation of the weather forecast has been gaining momentum with the development of irrigation system, which is a decision support system (DSS), and is built on the basis of online, open-source tools to supply instruction for irrigation water management [16]. While the use of weather forecast would improve water productivity, it is inherently uncertain, particularly for the rainfall. Previous studies usually utilized weather forecast data directly for long term without using actual weather data or made the irrigation decision based on historical weather data. By carrying out update run using actual weather data downloaded from nearby weather station, we may minimize the negative effects of errors in weather forecast.

Although the use of sensors and models have made the irrigation system more water-saving, the efficiency in nutrient use under different irrigation schemes should also be evaluated, because inefficient practices usually lead to increase in nutrient leaching, especially in the sandy loam soil [17]. Wang et al. [18] simulated three Christiansen uniformities of drip irrigation using HYDRUS-2D, and demonstrated that deep percolation and nitrate leaching usually happened following a heavy precipitation event. Additionally, sandy loam soil is more susceptible to nitrate leaching than silty loam [19]. Actually, for most of the irrigation system, root, as the main nutrient and water absorbing organ and grows constantly, was often neglected or too simplified in the numerical models [20].

In this study, with the target of maximize net income, and simulate plant growth using specific plant parameters, the irrigation depths were determined by predicting two points of cumulative transpiration at each irrigation event, using actual weather records and WF to update and optimize the simulation. To validate this scheme, field experiments using potato were carried out for two-seasons, and the new scheme was compared with two other conventional irrigation strategies: automatic and refilling schemes. The objectives of this study were to: (1) investigate the feasibility of the proposed irrigation-depth-decision scheme which aims to maximize net income for potato, in comparison with the automated irrigation system managed with tensiometers and refilling irrigation scheme supplying full crop water requirement; (2) evaluate the nitrogen uptake efficiency and nitrate leaching during the irrigation period. Results of this study may contribute to the development of a new irrigation scheme which determines irrigation depths for maximizing net income of farmers and improving water management in water scarce area.

2. Material and Methods

2.1. Maximization of Virtual Net Income

To maximize the net income of farmers and develop sustainable water management in agriculture, Fujimaki et al. [21] proposed an irrigation scheme that determined irrigation depth by maximizing virtual net income, I_n (\$ ha^{-1}) and priced water. Though the net income cannot be achieved until final harvest, we assume that virtual net income is proportional to the cumulative dry matter (DM) accumulated during an irrigation interval, because plant dry matter accumulation is usually correlated with cumulative transpiration, as both CO_2 uptake and water vapor loss take place simultaneously via stomata [21–23]. For the economic yield of crop which contributes to the net income, such as fruit, grain, tuber, is assumed to be proportional to dry matter production. In other words, harvest index, which is defined as edible to entire biomass, is assumed to be constant. Then, cost for water usage and other costs are subtracted from income, presuming that water is volumetrically priced to give incentive to farmers to save water. Thus, the I_n, during an interval is calculated as:

$$I_n = P_c \xi \varepsilon \tau_i k_i - P_w W - C_{ot} \quad (1)$$

where P_c is the producer's price of the crop (\$ kg^{-1} DM), ξ is the harvest index, ε is transpiration efficiency of the crop which is produced DM (kg ha^{-1}) divided by cumulative transpiration (kg ha^{-1}), τ_i is cumulative transpiration during an irrigation interval (1 cm = 10^5 kg ha^{-1}), k_i is the income correction factor, subscript i is specific irrigation interval, P_w is the price of water (\$ kg^{-1}), W is the irrigation depth (1 cm = 10^5 kg ha^{-1}), and C_{ot} is other costs during the period such as fertilizers and pesticide, etc. (\$ ha^{-1}).

To avoid an underestimation of the contribution of I_n during the initial growth stage, during which transpiration rate is far smaller compared with later growth stage but equally important in produce economic yield. Thereafter, a correction function of k_i was set based on the basal crop coefficient [21]. Although the introduction of k_i will not make I_n correspond to the actual net income even the prediction of yield matches the actual well, it may enhance the accuracy of virtual I_n. It was defined as follows:

$$k_i = \frac{\overline{k}_{cb}}{k_{cb}} = \frac{\int k_{cb} d\tau}{\tau_f k_{cb}} = \frac{\left(a_{k_{cb}} + c_{k_{cb}}\right)\tau_f - \frac{a_{k_{cb}}}{b_{k_{cb}}}\left[\exp\left(b_{k_{cb}}\tau_f\right) - 1\right] - \frac{d_{k_{cb}}\tau_f^{e_{k_{cb}}+1}}{e_{k_{cb}}+1}}{\tau_f k_{cb}} \quad (2)$$

where $\overline{k}_{cb}$ is average values of basal crop coefficient (k_{cb}) across growing period; τ_f is expected cumulative transpiration at final period; $a_{k_{cb}}$, $b_{k_{cb}}$, $c_{k_{cb}}$, $d_{k_{cb}}$ and $e_{k_{cb}}$ are fitting parameters used to calculate basal crop coefficient as a function of cumulative transpiration as described later.

Fujimaki et al. [21] empirically described the τ_i as

$$\tau_i = \int T_r d_t = a_t[1 - \exp(b_t W)] + \tau_0 \quad (3)$$

This nonlinear relationship requires three runs of heavy two-dimensional simulation of water flow to get optimum irrigation depth, which is somewhat time consuming. To reduce the number of trials, Abd EI Baki et al. [22] proposed a simpler function to describe the relationship between W and τ_i, composed of two linear functions, which requires two runs, skipping the third run. The function assumes that τ_i linearly increases with W until the potential transpiration (τ_{max}) is obtained, as follows:

$$\tau_i = \int T_r dt = a_t W + \tau_0,\ W < \frac{\tau_{max} - \tau_0}{a_t} \quad (4)$$

$$\tau_i = \tau_{max},\ W > \frac{\tau_{max} - \tau_0}{a_t} \quad (5)$$

where T_r is actual transpiration rate (cm s^{-1}), a_t is a fitting parameter, τ_0 is τ at no irrigation.

2.2. Determination of Optimum Irrigation Depth

The optimum irrigation depth, which gives maximum I_n, is obtained when derivative of Equation (1) with regard to W become zero:

$$\frac{dI_n}{dW} = a_t P_c \varepsilon k_i - P_w,\ W < \frac{\tau_{max} - \tau_0}{a_t} \tag{6}$$

$$\frac{dI_n}{dW} = -P_w,\ W > \frac{\tau_{max} - \tau_0}{a_t} \tag{7}$$

In the range of $a_t P_c \varepsilon k_i - P_w \geq 0$, the optimum W is $\frac{\tau_{max} - \tau_0}{a_t}$ (Equation (6)). While in the range of $a_t P_c \varepsilon k_i - P_w < 0$, I_n decreases with W (Equation (7)) and no irrigation is recommended. In the scheme, τ_0 and a_t are determined by two trials at W = 0 and W_1. Because the cumulative transpiration during the irrigation interval under irrigation should be between τ_0 and ET_0, and additional water is somewhat required to compensate evaporation loss W_1 is set at half of τ_0 + ET_0. Thereafter, α_t was determined by the two points in the linear Equation (4), (0, τ_0) and ((τ_0 + ET_0)/2, τ_1).

2.3. Numerical Model

The proposed scheme in Section 2.1, Section 2.2 and a graphical user interface for entering parameter values have been embedded into a numerical model, WASH_2D, which simulates the two-dimensional movement of water, heat and solute in soils with the finite difference method [21]. This scheme partitions crop evapotranspiration (ET_c) into two components, actual evaporation and actual transpiration, where actual evaporation was calculated using bulk transfer equation and was described by Fujimaki et al. [21], and actual transpiration was described in the following. The software used in this study can be freely downloaded with source code under a general public license from https://www.alrc.tottori-u.ac.jp/fujimaki/download/WASH_2D, accessed on 26 September 2022.

The actual transpiration rate, T_r, is computed by integrating the water uptake rate, S (cm s^{-1}), over the root zone [24]:

$$T_r = L_x^{-1} \int_0^{L_x} \int_0^{L_z} S d_x d_z \tag{8}$$

where L_x and L_z are the width and depth of the calculated root zone, respectively. The S was described as follows:

$$S = \alpha_w \beta T_p \tag{9}$$

where α_w, β, and T_p are reduction coefficient, normalized root density distribution, and potential transpiration rate (cm s^{-1}), respectively. The α_w is a function of matric (φ, cm) and osmotic potential (φ_o, cm), which is called stress response function. WASH_2D uses an additive form stress response function:

$$\alpha_w = \frac{1}{1 + \left[\frac{\varphi}{\varphi_{50}} + \frac{\varphi_o}{\varphi_{o50}}\right]^p} \tag{10}$$

where φ_{50}, φ_{o50}, and p are fitting parameters [25]. The φ_{50} and φ_{o50} are heads when water uptake is decreased to 50% of its potential rate and therefore represent simple indices of the tolerance of crops.

The root activity, β, is described as [21]:

$$\beta = 0.75(b_{rt} + 1) {d_{rt}}^{-b_{rt}-1} (d_{rt} - z + z_{r0})^{b_{rt}} g_{rt} \left(1 - x^2 {g_{rt}}^{-2}\right) \tag{11}$$

where b_{rt} is a fitting parameter; d_{rt} and g_{rt} are the depth and the width of the plant root zone (cm), respectively; g_{rt} was set 20 cm according to the potato experiment we conducted in same site in 2020; z and z_{r0} are the soil depth and the depth below which the roots exist (cm), respectively; x is horizontal distance from the plant (cm). The d_{rt} is expressed as function of cumulative transpiration from germination, τ, as follows:

$$d_{rt} = a_{drt}[1 - \exp(b_{drt}\tau)] + c_{drt} \tag{12}$$

where a_{drt}, b_{drt}, and c_{drt} are fitting parameters.

T_p is calculated by multiplying the reference evapotranspiration rate (ET_0, cm s^{-1}) with basal crop coefficient (k_{cb}) as follows:

$$T_p = ET_0 k_{cb} \tag{13}$$

The ET_0 was calculated using Penman-Monteith equation [26] into which measured data in weather stations or weather forecast data were input. The k_{cb} is calculated as a function of τ as follows [27]:

$$k_{cb} = a_{k_{cb}}\left[1 - \exp\left(b_{k_{cb}}\tau\right)\right] + c_{k_{cb}} - d_{k_{cb}}\tau^{e_{k_{cb}}} \tag{14}$$

where $a_{k_{cb}}$, $b_{k_{cb}}$, $c_{k_{cb}}$, $d_{k_{cb}}$, and $e_{k_{cb}}$ are fitting parameters, and the last term stands for the decline at last growth stage.

To make the plant growth dynamically respond to drought and salinity stresses, k_{cb} and d_{rt} were expressed as function of τ rather than calculate according to days after sowing. The values of these parameters are listed in the following section (Section 2.5 (b)).

2.4. Simulation Procedure

The procedure to determine the irrigation depth in proposed scheme is shown in Figure 1. For update produce, (1) the process began with downloading the last two days' weather data from weather station and preparing irrigation records file to set the atmospheric boundary condition, and water content profile at the end of the last update run as the initial condition in water flow module to perform a numerical simulation to update the soil water distribution. Left boundary condition and lower boundary condition were set as impermeable and gravitational flow, respectively. (2) Regarding solute movement module, the file containing solute concentration distribution output at the end of the last update run was input as initial condition, then, the concentration of infiltration water was input as upper boundary condition while zero concentration gradient was set as lower boundary condition. (3) Lastly, the cumulative transpiration was input in plant properties module to set as initial value.

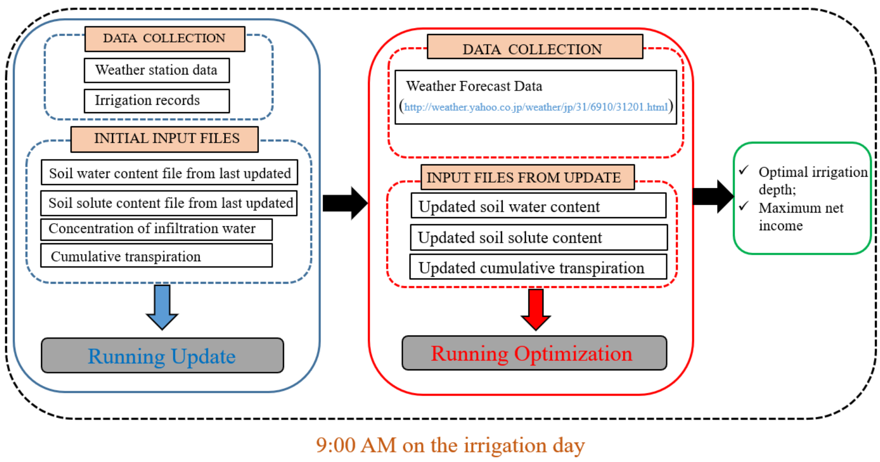

Figure 1. Steps of the proposed irrigation depth determination schedule. Two main steps (Running Update and Optimization runs) were performed by WASH_2D at 9:00 AM of the irrigation day. Left blue box shows the first step of simulation (Update). The right red box shows the second step of simulation (Optimization). The black arrow between two boxes shows the directions of data flow.

Then, optimization procedure was carried out as follows: (1) the updated soil water distribution file and solute concentration distribution file output from the update run were input as initial condition in water flow module and solute movement module, respectively. Then, (2) weather forecast data (average air temperature, relative humidity, wind speed, solar radiation, and rainfall) until the next scheduled irrigation were input as atmospheric boundary condition to get optimized irrigation depth for that irrigation day. Other settings were the same as update procedure.

2.5. Field Experiment

(a). Treatments

Field experiments using potato were carried out for two-seasons at Arid Land Research Center (ALRC), Tottori, Japan, in 2021. Three treatments were established: (1) Automated irrigation (Treatment A), based on soil suction monitoring; (2) Refilling irrigation (Treatment R) to recharge simulated volumetric water content in the root zone to field capacity, which may correspond to meeting potential evapotranspiration from last irrigation; (3) proposed scheme (Treatment S1 in first season and S2 in second season). Each treatment had three replicates. Each replicate was established on a drainage lysimeter with a 2 m long, 2 m wide and 2 m deep, filled with the local sandy soil. The soil hydraulic properties of experiment site were shown in Figure 2, which was measured by [21]. At the bottom of each lysimeter, a small tube to discharge drainage water was installed as depicted in Figure 3. In this study, we measured the amount of drainage for each treatment by installing an ECRN-50 Rain Gauge (METER Inc., Pullman, Washington, DC, USA). To evaluate the nitrate concentration (NO_3-N) in the drainage water, a plastic cup was set under the Rain Gauge to collect water per week (first season) and per two days (second season). The NO_3-N concentration was measured with IC_SI-90 4E (Shimadzu Corporation, Kyoto, Japan).

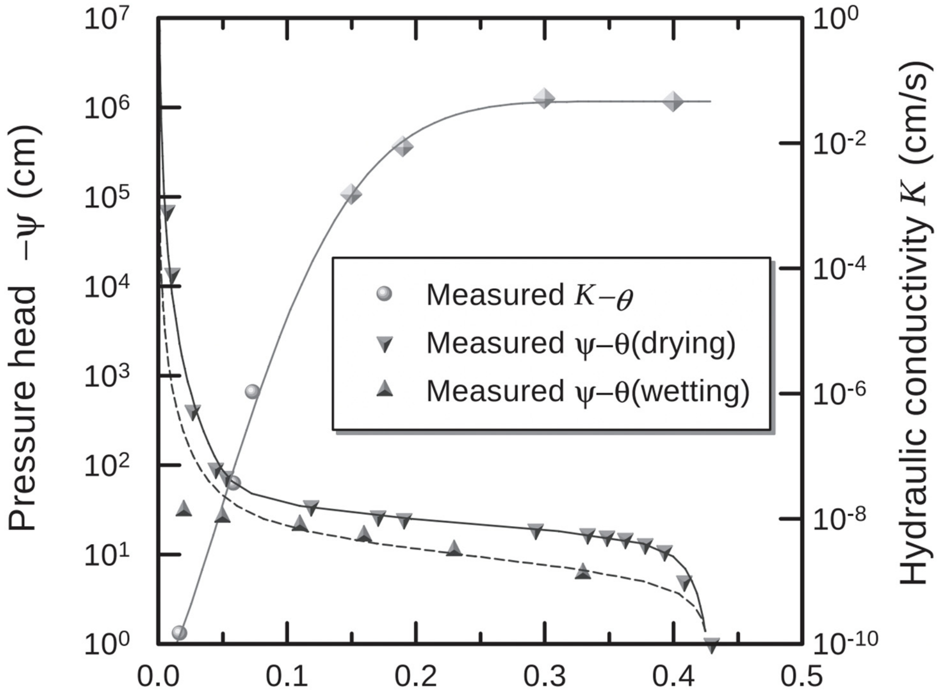

Figure 2. Hydraulic properties of Tottori sand in the experiment site.

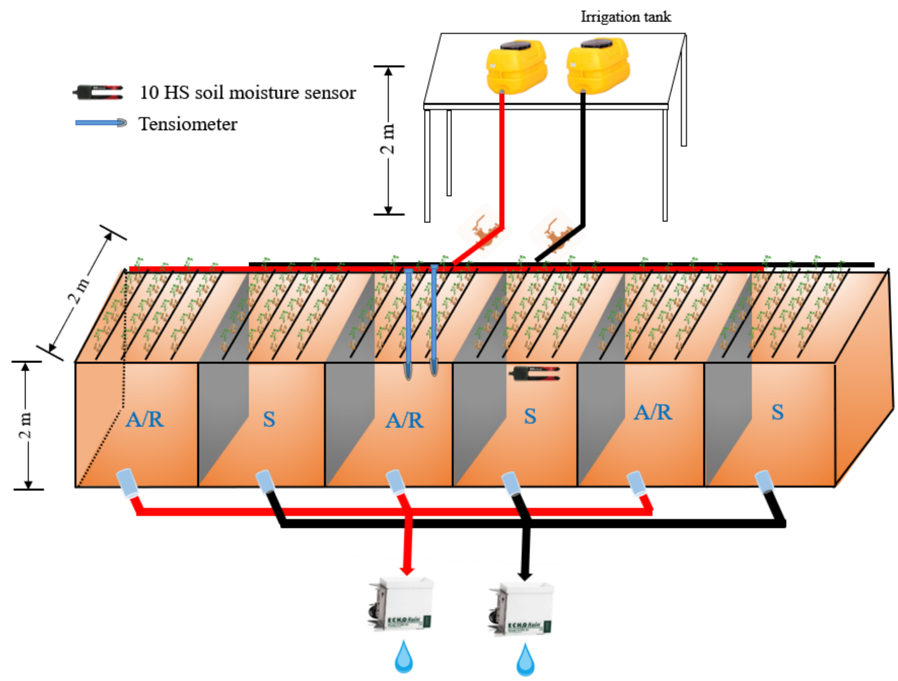

Figure 3. Schematic representation of the experimental setup. The red tube connected to left yellow water tank was arranged for irrigation of A/R plots and black tube connected to right side was for S plots (A/R stands for Automated irrigation in first season or Refilling treatment in second season, S stands for Schemed irrigation). There were four 10 HS sensors installed at different position of soil profile in the middle plot of S treatment (only one shown in Figure). Two 20 cm tensimeters were installed at the middle plot of A/R.

(b). Plant

Potato seed pieces about 30 g (*cv. Nishiyutaka*) were planted every 20 cm at a depth of 15 cm in row spaces 50 cm apart. The sowing, harvest time and total irrigation amount of two seasons were listed in Table 1. The potato sprouts germinated in four weeks after planting. The values of drought and salinity stress parameters (φ_{50} and φ_{050}) included in a widely used macroscopic root water uptake model [24,28], were determined by a cost-effective and reliable method presented by Fujimaki et al. [29] before the field experiment. Parameter values of stress response, normalized root density distribution and the depth of root zone functions of potato were listed in Table 2. We set the price of crop at 1 (\$ kg^{-1} DM) by referring to the prices received by producers in the USA in 2011 (FAOSTAT, http://faostat.fao.org/) (accessed on 26 September 2022) and set price of water at 0.00025 \$ kg^{-1} [30]. The parameter values of crop coefficient in Equation (14) were determined by fitting K_{cb} value and cumulative transpiration amount. The K_{cb} value of potato were derived in Table 17 of Allen et al. [26], and daily K_{cb} value was determined by dividing the growing period into four general growth stages and selecting and adjusting the K_{cb} value corresponding to the initial, mid-season and end of late season stages. Meanwhile, according to the local weather condition, the average ET_0 value during initial, development, mid and last stage were set as 3, 4, 5, 5 mm d^{-1}, respectively. The fitting curve is drawn in Figure 4. During the growing period, leaf area index (LAI) and above ground biomass (g plant^{-1}) were measured four times at key stages. At harvesting, the aboveground fresh weight (FW) and belowground tubers were determined by harvesting all the plants from an area of 1 m^2 in each plot center, leaves, stems and tubers were separately measured. After recording their fresh weight, the samples of potato biomass were oven-dried at 105 °C for two hours and 65 °C to constant weight to determine their dry weight (DW). Subsequently, dried tuber, straw (leaf and stem) were pulverized with a micro plant grinding machine (BMS-A20TP, Biomedical Science Co., Tokyo, Japan) and then sieved manually through

0.5 mm mesh. The nitrogen content of each part was measured with CN coder (Micro Coder JM10, J-Science Lab Co., Tokyo, Japan).

Table 1. Dates of sowing and harvest as well as irrigation amount during two growing seasons of potato.

Seasons	Treatment	Dates of Sowing (m/d)	Dates of Harvest (m/d)	Growth Period (days)	Total Irrigation Amount (mm)
First season	A	19 March	July 17	120	286
	S1				207
Second season	R	27 August	December 8	103	99
	S2				115

Note: A stands for Automated irrigation, S1 stands for Simulated irrigation in first season, R stands for Refilling treatment, S2 stands for Simulated irrigation in second season.

Table 2. Parameter values for plant stress response and growth properties used in the numerical modeling in this study.

Parameter	Value	Remarks
P_w	0.00025	Equation (1)
P_c	1	
ε	0.002	
$a_{k_{cb}}$	1.03	Equations (2) and (14)
$b_{k_{cb}}$	-0.37	
$c_{k_{cb}}$	0.15	
$d_{k_{cb}}$	1.40×10^{-7}	
$e_{k_{cb}}$	4.6	
φ_{50} (cm)	-100	Equation (10)
φ_{050} (cm)	-8200	
p	2.9	
b_{rt}	1	Equations (11) and (12)
g_{rt}	20	
z_{rt}	1	
a_{drt}	40	
b_{drt}	-4	
c_{drt}	10	

Note: the meaning of each parameter was explained in corresponding formula site.

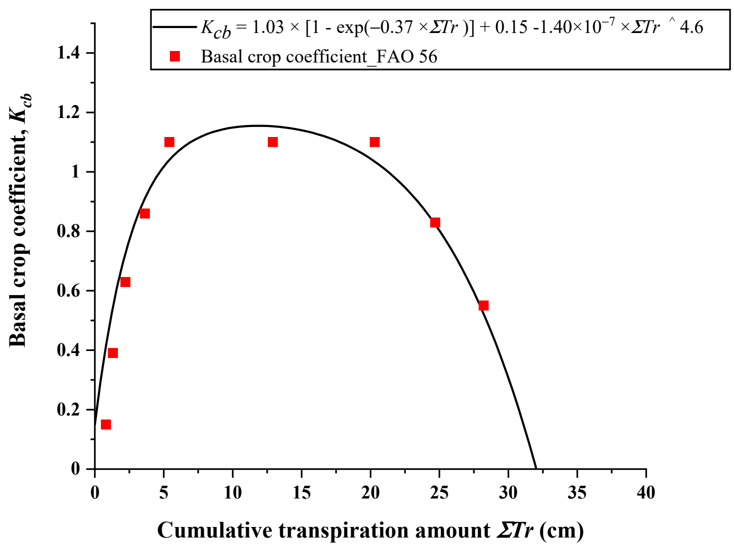

Figure 4. The basal crop coefficient (K_{cb}) of potato as a function of cumulative transpiration ($\sum Tr$) (parameter values of K_{cb} function were obtained by fitting to values reported by Allen et al. (1996).

(c). Irrigation and fertilizer

Four drip irrigation tubes with a discharge rate of 1 L h^{-1} per emitters were set in each plot, and the lateral and emitter distance spaced as 50 cm and 20 cm respectively as depicted in Figure 3. Irrigation interval for S and R was set at two days, because the field capacity of the sandy soil in experiment site was only 0.09 cm^3 cm^{-3}. Automated irrigation was triggered when the average readings of two tensiometers installed at the depth of 20 cm around plant was over than 45 cm, which was slightly higher than suction at field capacity and suitable for crop growth in sandy soil. To check the accuracy of volumetric water content (VWC) of the model simulated, four 10HS sensors (METER Inc., Pullman, Washington, WA, USA) were inserted into the soil profile at 4 observation points (x, z): (0, 5), (0, 45), (10, 10), (25, 5), respectively, where x is the horizontal distance (cm) from drip tube. The calibration function of 10HS sensor is shown in Figure 5. Composite liquid fertilizer with N-P-K at 8%-4.3%-4.2% was supplied with irrigation water by applying constant amount per irrigation event, while granular fertilizer N-P-K at 8%-3.5%-6.6% was supplied at tuber filling stage. The total N supplied was 152 and 155 kg ha^{-1} for A and S1 in the first season, and 97 and 99 kg ha^{-1} in the second season for R and S2, respectively. The reason for less supplement of fertilizer in second season was frequent rainfall and decreased air temperature, which reduced irrigation times.

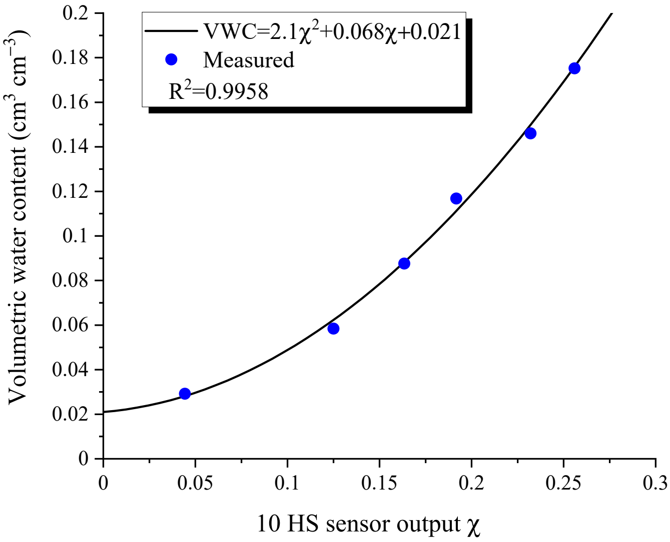

Figure 5. Calibration function for 10 HS sensor in sandy soil in experiment plot.

(d). Weather data

Weather data was collected from weather station located at 50 m away from the field. Weather forecast data was downloaded by a utility program (WeatherForcestDownloader, available from our website: http://www.alrc.tottori-u.ac.jp/fujimaki/download/WeatherForcestDownloader) (accessed on 26 September 2022), which can be used to extract 2 days of local WF data from the website of Yahoo! Japan (http://weather.yahoo.co.jp/weather/jp/31/6910/31302.html, accessed on 26 September 2022). Solar radiation data is not included in this website, instead, classes of cloud such as "rain", "cloudy", or "clear" were provided. To obtain the exact solar radiation value, an empirical relationship, 1-0.006 × cloud cover (%) (cloud cover (%): "clear" = 82%, "cloudy" = 63%, and "rain" = 32%), was multiplied by extraterrestrial radiation [21].

2.6. Nitrogen Uptake Efficiency

Plant nitrogen uptake were calculated using the following equations:

$$N_{uptake} = N_{tuber}Y_{tuber} + N_{straw}Y_{straw} \quad (15)$$

$$NU_pE = N_{uptake}/N_{supply} \quad (16)$$

where N_{uptake} is nitrogen uptake (kg ha^{-1}); N_{tuber} and N_{straw} are nitrogen content in tuber and straw (kg kg^{-1}), respectively; Y_{tuber} and Y_{straw} are biomass yields of tubers and straw (kg ha^{-1}), respectively; Where NU_pE is nitrogen uptake efficiency (kg ha^{-1}); N_{supply} is total nitrogen supplied during crop growth period (kg ha^{-1}).

To evaluate the nitrate content of each soil layer, soil samples at different depths (0–50 cm, 10 cm as increment) were collected. Each treatment had three replicates, and the nitrate content in the fresh soil were extracted with 1 M KCl (20 g soil: 100 mL KCl solution) and quantified at 220 nm using UV spectrophotometer (UV-1900i, SHIMADZU Co., Kyoto, Japan). The nitrate nitrogen stocks (NNS) at different soil depths were calculated using following equations:

$$NNS_i = NNC_i \times BD_i \times D_i \times 0.1 \; (\mathrm{i}_{1,2,3,4,5} = 0\text{–}10,\ 10\text{–}20,\ 20\text{–}30,\ 30\text{–}40,\ 40\text{–}50) \quad (17)$$

$$NNS_{0-50} = NNS_{i1} + NNS_{i2} + NNS_{i3} + NNS_{i4} + NNS_{i5} \quad (18)$$

where NNS_i and NNC_i are nitrate nitrogen stock (kg ha^{-1}) and nitrate nitrogen content (mg kg^{-1}) at the different soil layer (0–50 cm) respectively. BD_i is bulk density (g cm^{-3}) at the different soil layer, D_i is depth of each layer (m).

The nitrate leaching in each of the two seasons was determined by multiplying the nitrate concentration in soil solution with the drainage volume. The nitrate concentration during two sample periods were determined by linear interpolation method.

2.7. Soil Water Balance Equation

The soil water balance equation used for estimating actual evapotranspiration (ET_a) is as follows:

$$ET_a = P + I + SWD - D \quad (19)$$

where P is the cumulative precipitation from onset to end (mm); I is the cumulative depth of irrigation from onset to end (mm); SWD is soil water depletion from onset to end (mm); D is drainage amount (mm).

2.8. Statistical Analysis

The experiment was conducted with three treatments and three replicates per treatment. Data are presented in graphs and tables as means of three replicates, whereas in the graphs the standard. One-way ANOVA was conducted to analyze different factors among different treatments. The least significant difference (LSD) test ($p < 0.05$) was conducted when the differences were significant. Figures were created using OriginPro 2020 (OriginLab Inc., MA, USA). The performance of model was evaluated using the root mean square error (RMSE) of VWC, which was calculated as follows:

$$RMSE = \sqrt{\sum_{i=1}^{n}(x_i - y_i)^2/n} \quad (20)$$

where n is the number of measured or simulated data; x_i is the measured VWC; y_i is the estimated VWC.

3. Results and Discussion

3.1. Weather Conditions

The values of daily maximum temperature (T_{max}), daily minimum temperature (T_{min}), solar radiation (R_s) and mean relative humidity (RH_{mean}) of two growing seasons are shown in Figure 6. The mean maximum temperature was 21.7 and 22.2 °C, the mean minimum temperature was 13.7 and 14.9 °C, and the mean solar radiation was 13.3 and 8.0 MJ m^{-2} d^{-1} for the two seasons, respectively. The growing degree days (GDD) of potato was 1607.6 and 1419.8 °C in two seasons, respectively, which was acceptable for final harvest [31]. The RH_{mean} of 74.4% in first season and 74.8% in second season was similar. Lower R_s and temperature at tuber building period in second season affected the yield production.

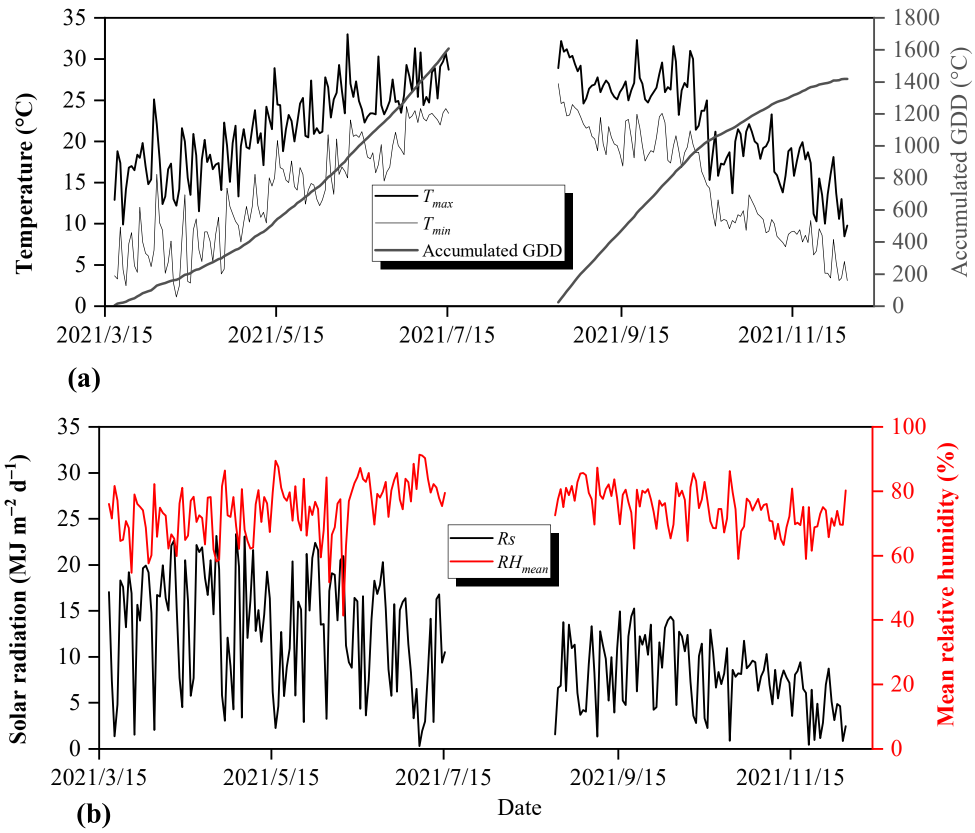

Figure 6. Meteorological condition from sowing to harvest of potato in two growing seasons in 2021. (**a**) daily maximum temperature, minimum temperature, and accumulated growing degree days (T_{max}, T_{min}, and Accumulated *GDD*, respectively), (**b**) solar radiation (R_s) and mean relative humidity (RH_{mean}). Accumulated GDD= [(T_{max} + T_{min})/2-4.4 °C], base temperature was set at 4.4 °C [32].

3.2. Soil Water Content Change

To evaluate the accuracy of model simulation, we compared the measured and simulated volumetric water content (VWC) of treatment S. The simulated VWC was derived from the result of update procedure at each irrigation event, where weather station data was input as upper boundary condition. Figure 7 shows the measured and simulated VWC change at the depth of 5 cm and 45 cm below the drip tube in two seasons. The RMSE of VWC at the depth of 5 cm (Figure 7a,c) during the two seasons were 0.018 and 0.024 m^3 m^{-3}, respectively, which indicates that WASH_2D model could simulate soil moisture change in fair agreement. However, model overestimated the VWC at the time when irrigation or rainfall just occurred. The reason of this overestimation would be because of an underestimation of hydraulic conductivity when the VWC at around 0.12 m^3 m^{-3}.

At the depth of 45 cm (Figure 7b,d), VWC significantly increased when there was a heavy or continuous rainfall, such as, April 29 and May 2 in the first season, and October 17, 23 in second season. The RMSE at the depth of 45 cm was 0.022 and 0.014 m^3 m^{-3} in the first and second season, respectively, indicating that simulated and measured VWC were in fair agreement at deep zone.

3.3. Evapotranspiration

To compare the simulated ET_c and measured ET_a, two periods in each season were chosen as shown in Figure 8. ET_c of automatic and refilling treatments were also simulated by entering irrigation records and actual weather data into the model to compare the outputs with measured data. Daily average ET_a calculated using Equation (19) were estimated between two heavy rainfall events, assuming the same VWC at field capacity in the root zone and hydrostatic profile in the deeper layer (0.09 m^3 m^{-3}) at one-day after heavy rainfall. The simulated ET_c in the first season was higher than measured ET_a, which might be mainly caused by the overestimation of basal crop coefficient growth This overestimation may be avoided by measuring basal crop coefficient as a function of cumulative transpiration. In the second season, the simulated ET_c agreed well with measured one. Overall, the RMSE between measured and simulated was 0.8 mm day^{-1}. In addition, we also compared the simulated daily ET_c of different treatments with ET_0. As shown in Figure 9, those of automated scheme was higher than those of simulated scheme in first season and has no difference in the second season. The cumulative ET_0 and ET_c of, S1, and A in the first season were 190, 175 and 189 mm, while those in the second season were 76, 70 and 67 mm for ET_0, S2 and R, respectively.

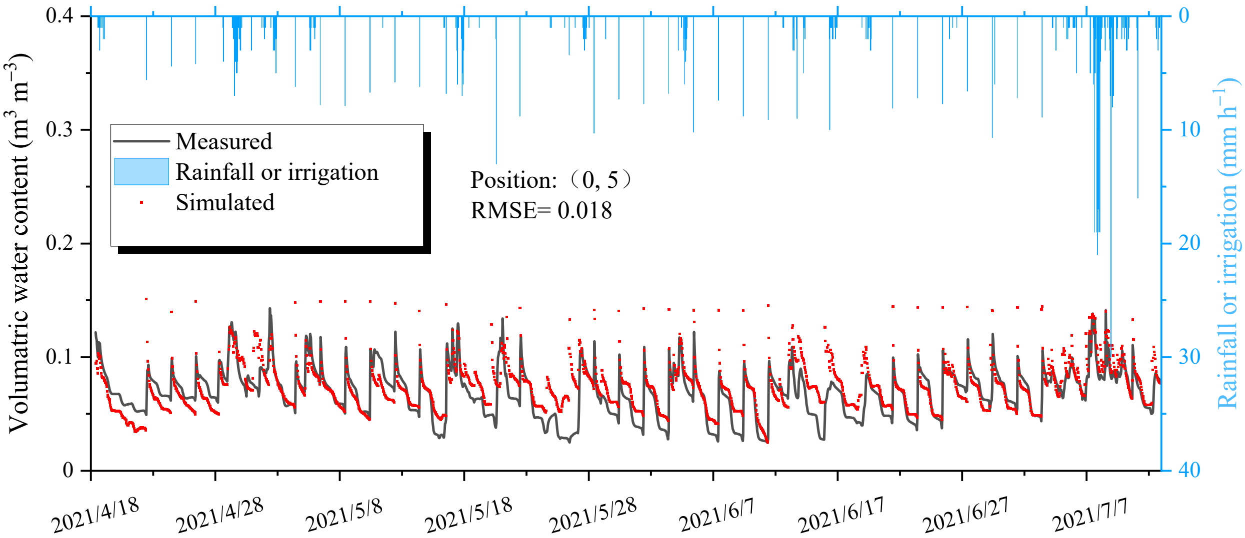

(a)

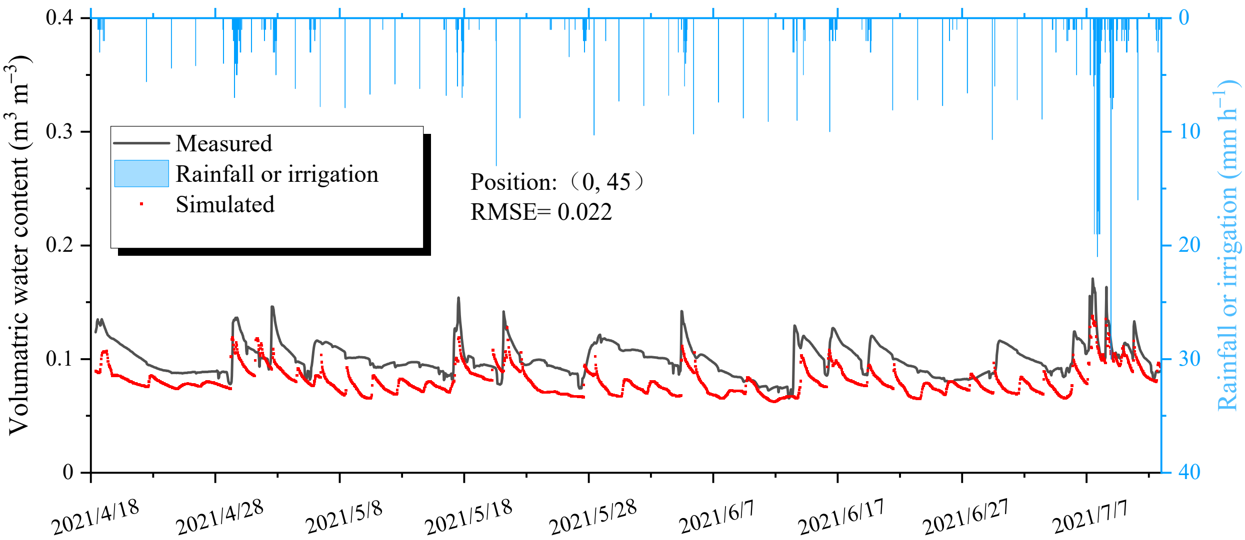

(b)

Figure 7. *Cont.*

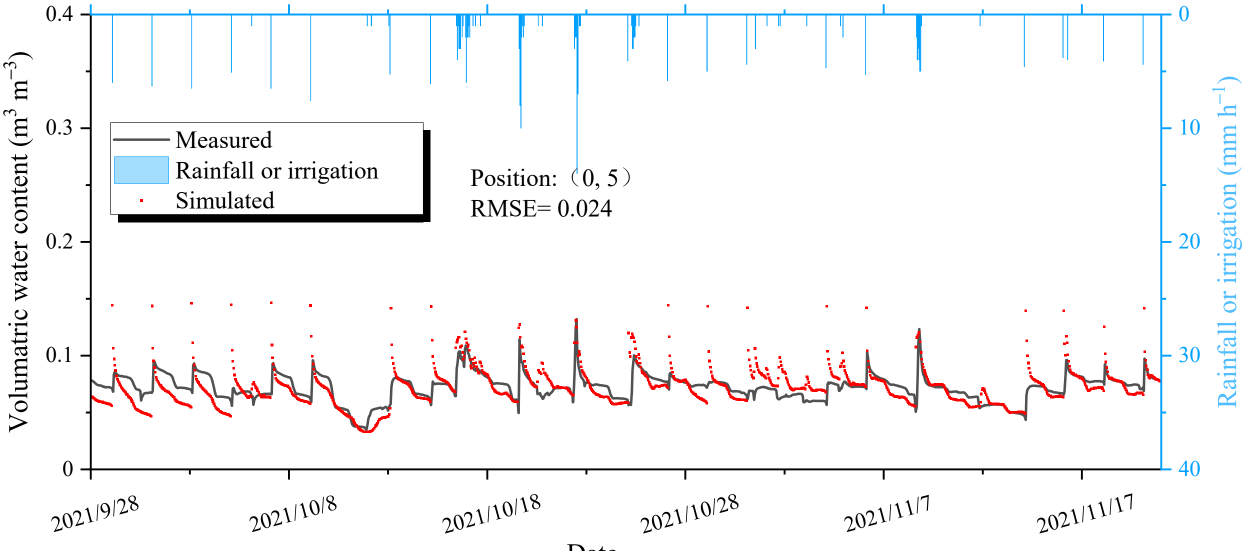

(c)

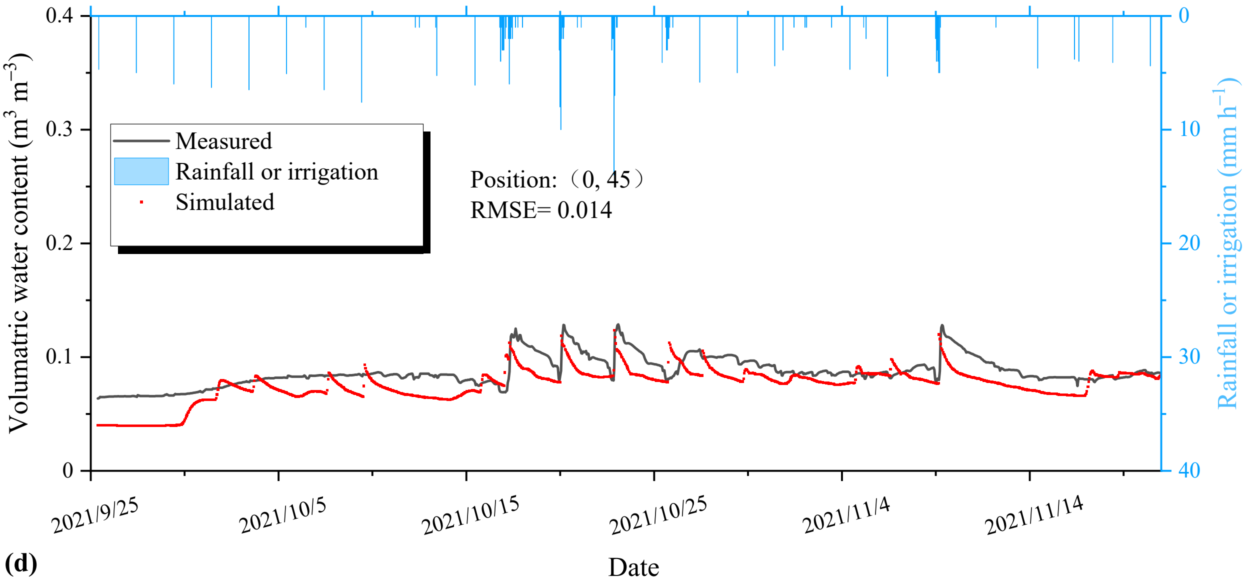

(d)

Figure 7. Comparison of simulated and measured VWC of treatment S at the depth of 5 cm and 45 cm below the drip tube in two seasons. (**a**,**b**) are the VWC at the site of (0, 5) and (0, 45) in the first season, respectively; (**c**,**d**) are the VWC at the site of (0, 5) and (0, 45) in the second season, respectively. RMSE is root mean square error.

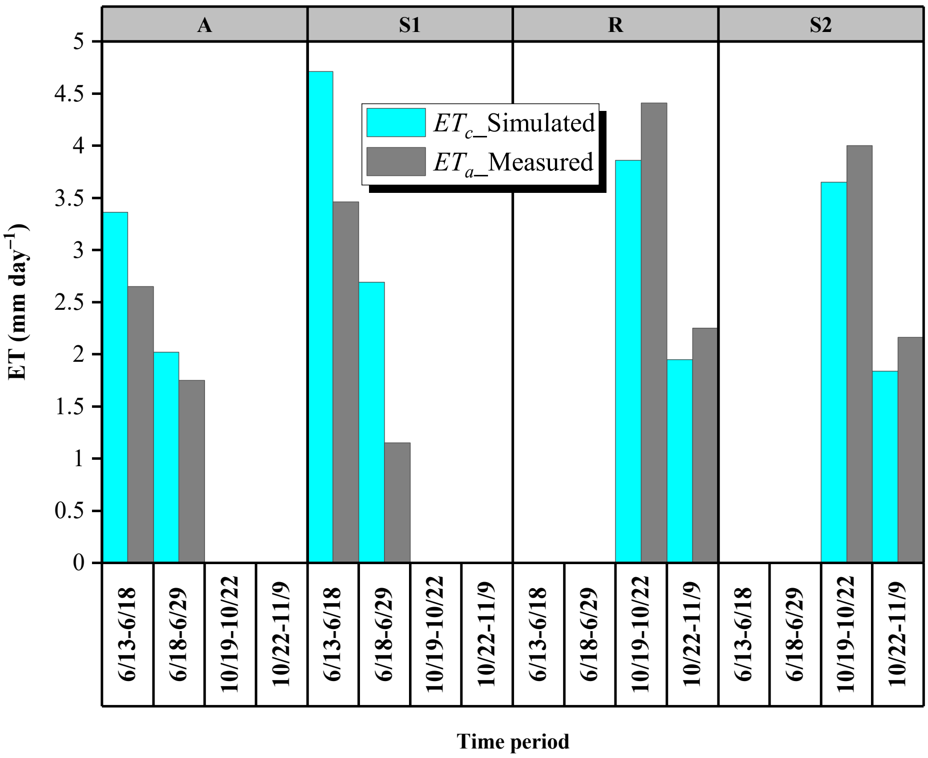

Figure 8. Comparison of measured ET_a and simulated ET_c under different treatment in two seasons. (6/13–6/18 and 6/18–6/29 time periods were chosen for the first season, 10/19–10/22 and 10/22–11/9 time periods were chosen for the second season).

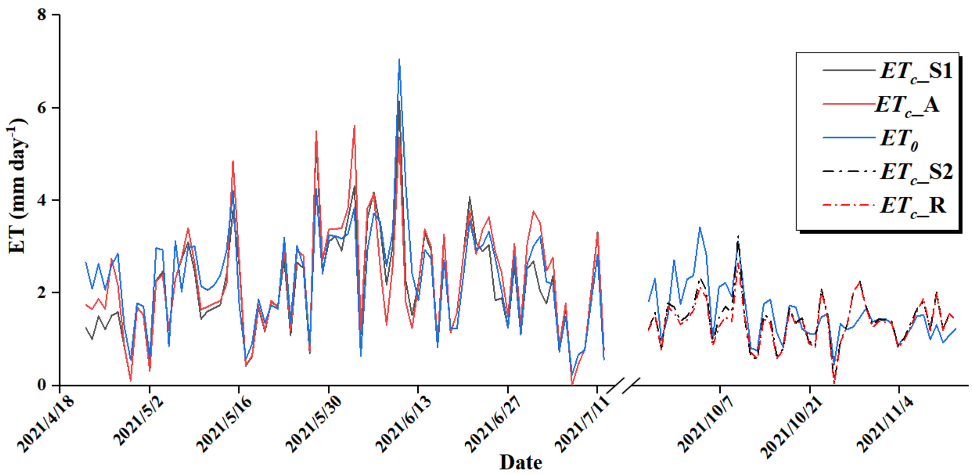

Figure 9. Time evolution of the reference ET (ET_0) and daily ET_c of different treatments during crop growth period in two growing seasons.

3.4. Growth of Potato

Figure 10 shows the LAI and above ground biomass (AGB) of potato measured in the two seasons. LAI and AGB are important indicators of crop growth, which determine the light interception capacity of the crop and photosynthetic accumulation of crop [33,34]. Both LAI and AGB had no significant difference at establishment and stolon initiation stage (15 < DAP < 40) in two seasons. But at the tuber initiation and filling stage (45 < DAP < 90), S1 and S2 were significantly higher than A and R in the first and second season, respectively, no matter for LAI or AGB. This situation might be due to higher nutrient utilization of S, especially nitrogen (N), a macronutrient that promotes carbon metabolism and plant growth, leading to biomass accumulation [35]. At the maturity stage (DAP > 90), both LAI and AGB decreased due to leaf senescence. It should be noted that the smaller canopy structure of potato in the second season led to delayed growth and reduced final yield, which mainly comes from low temperature and solar radiation during the critical growth stage.

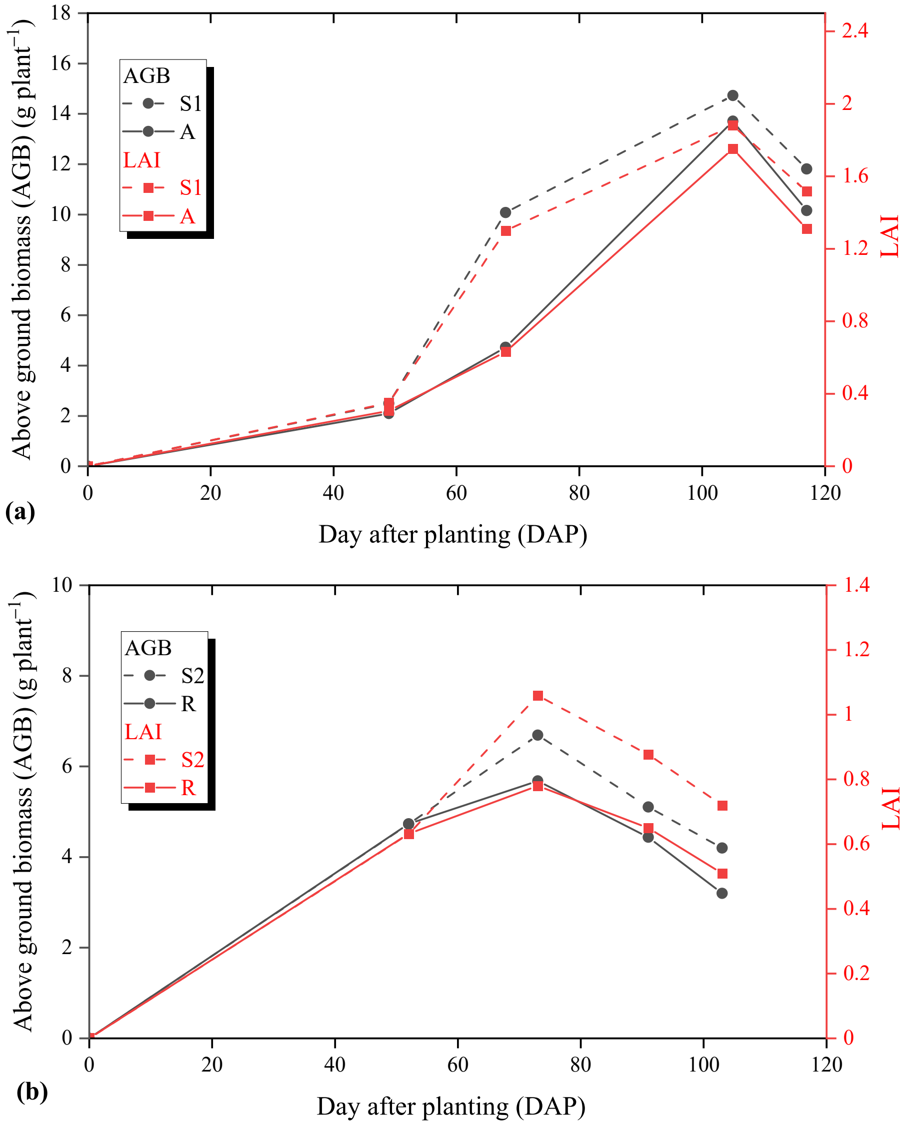

Figure 10. The time evolution of LAI and AGB for the potato under different treatments in first season (**a**) and second season (**b**).

3.5. Yield and Net Income

Figure 11 compares yield and net income of three different treatments in two seasons. We counted only cost for fertilizer only to calculate C_{ot} in Equation (1) by multiplying the total amount of fertilizers used and the price of the fertilizer. In the first season, the yield and net income of S1 were 19% and 19% higher than A, respectively. At the same time, S1 reduced 28% of irrigation water compared with A. These results coincide with the previous experiments by Abd EI Baki et al. [22] using corn. In the second season, S2 and R had no significant difference for both yield and net income. The yield and net income of schemed treatment in the second season was decreased by 41% and 41% compared with former season, respectively, and obtained similar values compared with R. The low temperature at maturity stage and solar radiation at whole growth stage (Figure 6) may have restricted the photosynthesis and lead to a lower production. Considering the water consumption and yield production at two seasons, proposed irrigation scheme saved water and improved farmers' net income.

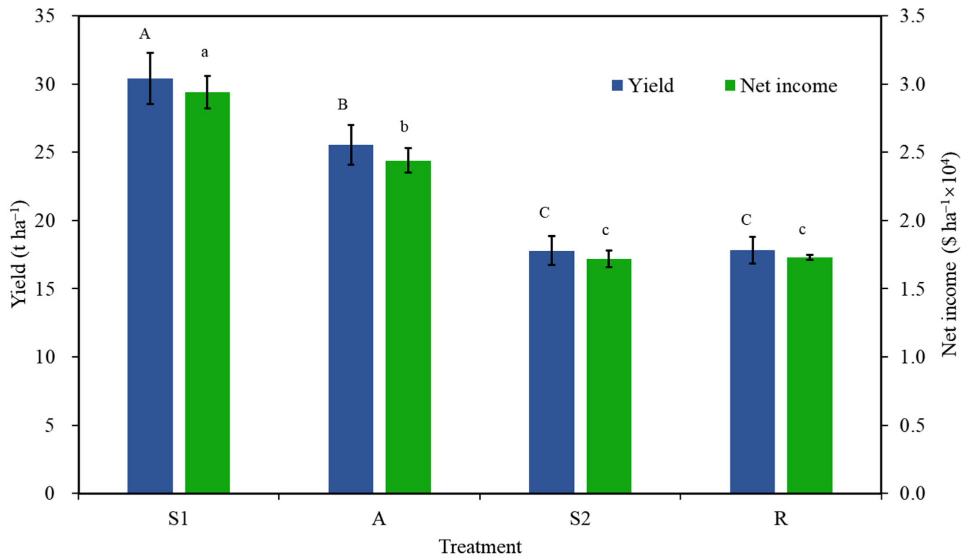

Figure 11. Comparison of yield and net income of different treatments in two seasons. (The error bars show the standard deviation of three replicates. The different uppercase letters indicating significant difference of yield under different treatments at $p < 0.05$, while the lowercase letters indicating significant difference of net income under different treatments at $p < 0.05$).

3.6. Nitrogen Uptake and Nitrate Leaching

The nitrogen storages in each part of potato are listed in Figure 12. The total nitrogen uptake for A and S1 in the first season were 138 and 182 kg ha^{-1} while that for R and S2 in the second season were 95 and 97 kg ha^{-1}. The NU_pE of S1 and S2 were 39% and 11% higher than A and R, respectively. Among that, the nitrogen storage in the tuber was the highest. The discrepancy of nitrogen uptake between two seasons was due to less nitrogen input and dry matter in the second season. The higher nitrogen uptake may have contributed to higher yield.

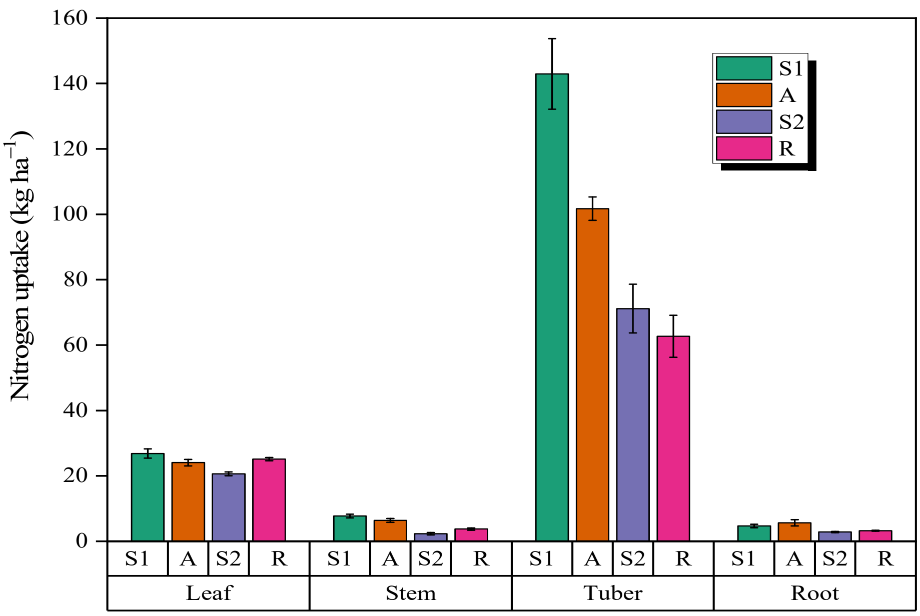

Figure 12. Nitrogen uptake of the different parts (Leaf, stem, tuber and root) of crop under different irrigation schemes in two seasons (The error bars show the standard deviation of three replicates).

As shown in Figure 13, the accumulative nitrate leaching at the outlet of the lysimeters of S1 and S2 were 105 and 54 kg ha^{-1}, which were 51 and 22% higher than A and R, respectively. The higher nitrate leaching in the first season is likely due to higher N supply and evenly distributed irrigation and precipitation. Though the total irrigation amount of A was higher than S1 in first season, the irrigation activities were concentrated in the early stage, while during late growth stage, less water was supplied due to large amount of rainfall. Such as from June 3 to 23, there was only 4.8 mm irrigation for A. Another possible reason is that frequent irrigation in treatment S increased the chance of nitrate leaching, while large amount of irrigation in treatment A for each time diluted the concentration of nitrogen. According to the results of this study, intensive irrigation might lead to nitrate leaching. In addition, we further analyzed the relationship between the nitrate leaching and water supply in terms of precipitation plus irrigation during second season (Figure 14). The linear regression can describe the relationships well between precipitation plus irrigation and nitrate leaching (R^2 = 0.80). Huang et al. [36] also reported similar relationship between monthly precipitation plus irrigation and monthly nitrate leaching. The accumulated soil nitrate after crop harvest matched the accumulative nitrate leaching. Higher accumulated soil nitrate of A and R (550 and 78 kg ha^{-1}) coincide with lower nitrate leaching in the two seasons, respectively. Furthermore, we also measured the soil nitrate content at different soil depths to evaluate the soil nitrate distribution at root zone (Figure 15). The nitrate content of A changed from 5.1 to 10.8 kg ha^{-1} at 0–50 cm soil layer in first season, higher than that of S1 except for the depth of 30–40 cm. The same trend was obtained in the second season, nitrate content of R ranged from 8.0 to 14.3 kg ha^{-1}. The increment of soil nitrate content in the second season might be due to decreased amount of precipitation plus irrigation (average 297 mm) compared with the first season (average 807 mm), resulting in a decrease in nitrate leaching and an increase in soil nitrate stock.

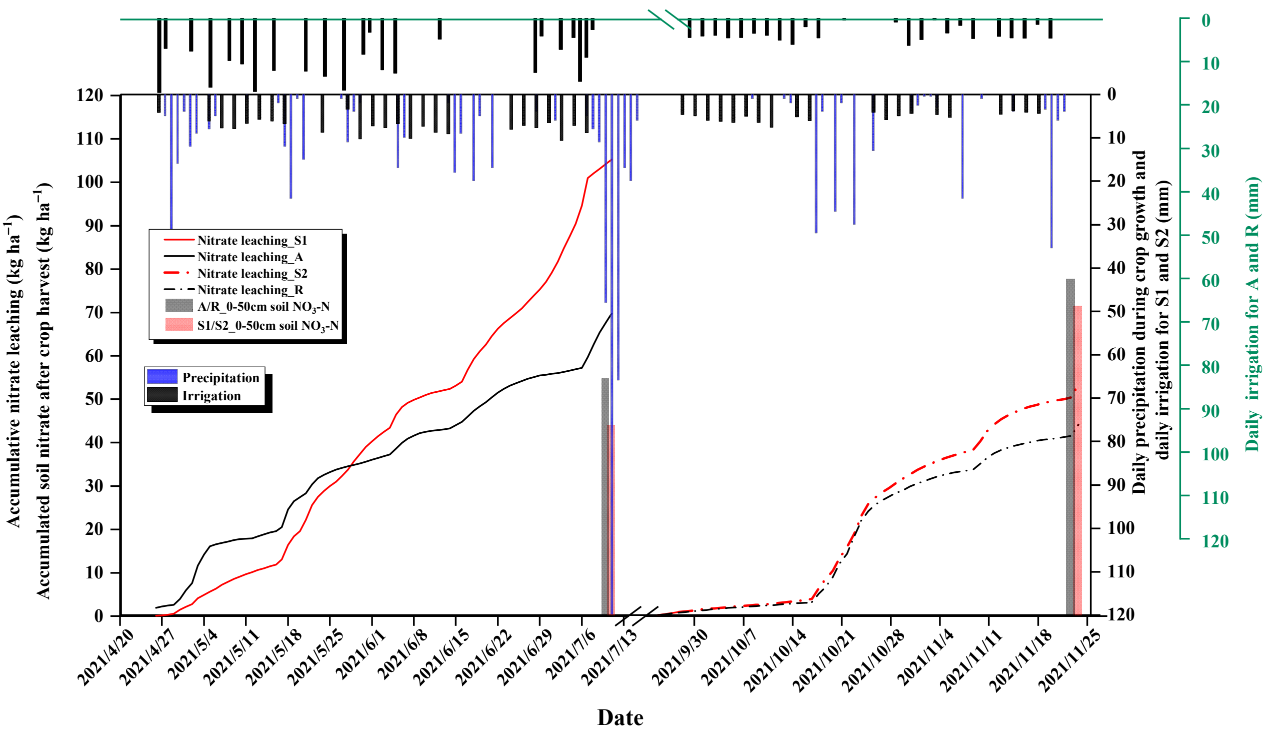

Figure 13. Accumulative nitrate leaching (2 m soil depth) during the growing period and accumulated soil nitrate content after crop harvest at 0–50 cm root zone depth (left axis); Daily precipitation amount in two seasons and daily irrigation amount for S1, S2, A and R (S1 and S2 using inner right axis, while A and R using outer right axis).

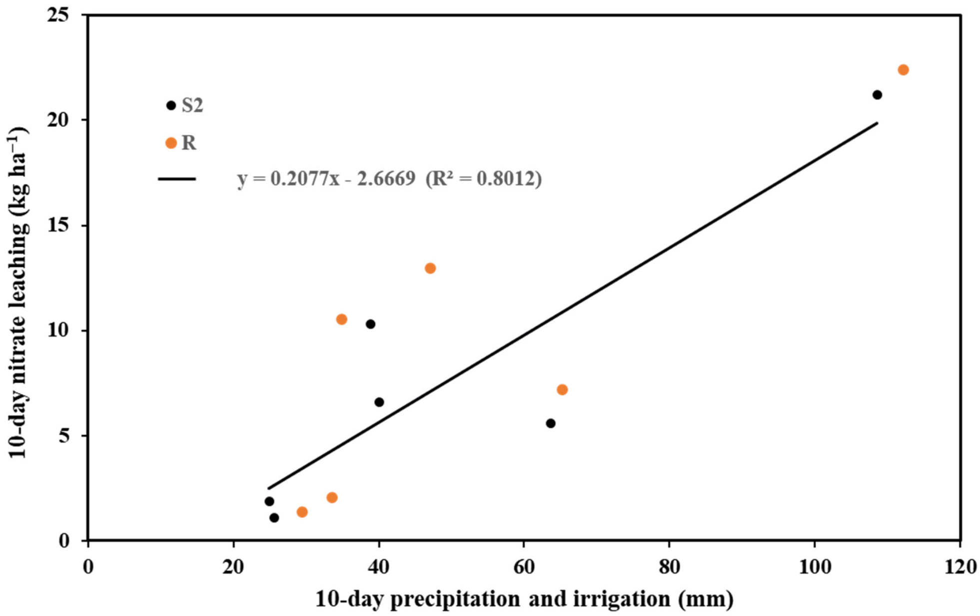

Figure 14. Linear regression between 10-day precipitation plus irrigation and 10-day nitrate leaching at 2 m soil depth in second season.

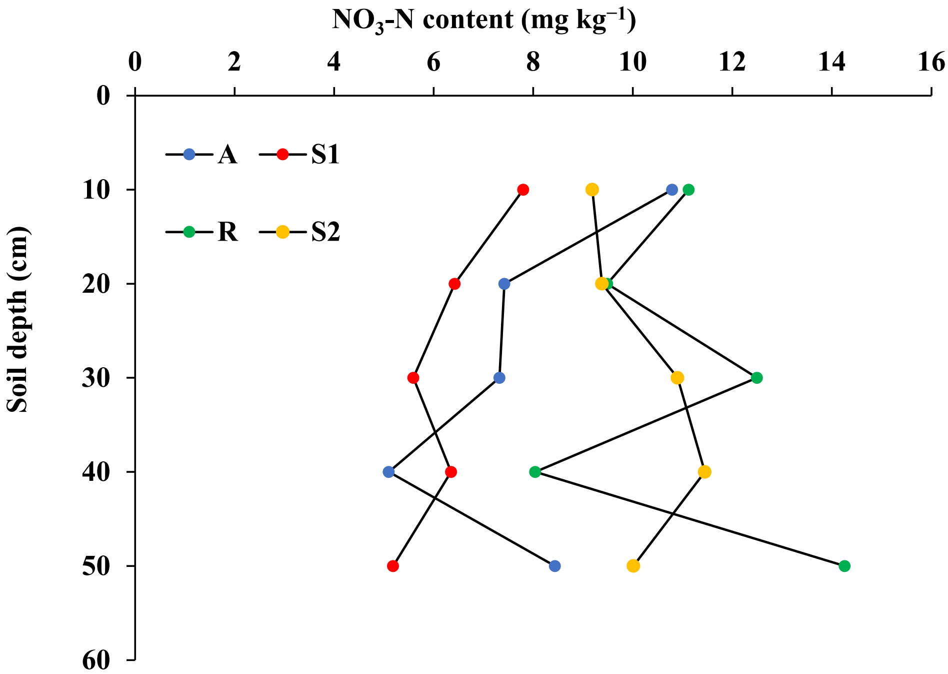

Figure 15. Soil NO_3-N content at different soil depths under different treatments in two seasons.

3.7. Accuracy of Weather Forecast

The accuracy of weather forecast has a large effect on the performance of model simulation. Figure 16 compares between observed weather data from weather station and forecast weather data. Because WF does not include data beyond 24:00 of the second day, we discard time period during night (from 0:00 to 9:00). The average temperature and relative humidity, as primary inputs weather data in model, matched well with measure data, with the RMSE of 1.7 °C and 10.2%, respectively. The rainfall, as an indirect factor modifying many of the crop growth and developmental processes [37], with the RMSE of 9.5 mm, which was not matching well with the measured data and may affect the recommendation of irrigation depths from model. For example, on June 19, 16 mm rainfall was forecast and therefore no irrigation was recommended from model, but actually no rain occurred (Figure 13). This situation may lead to temporary drought stress on crop. Although there was a large difference between the rainfall amount of weather forecast and measured one, the derived parameter, ET_0, calculated by forecasted data were in fair agreement with the measured ones, with an RMSE of 0.9 mm, which was acceptable. Since the accuracy of ET_0 is important to optimize irrigation depth as explained in Equations (1), (8), (9) and (13), if the prediction of ET_0 is within the acceptable range, the first term of Equation (1) could be estimated in fair accuracy. In addition to advance in climatology and steadily increasing speed and memory of super computers used for running general circulation models, deep learning model is being used to improve the accuracy of weather forecast model such as European Centre for Medium-Range Weather Forecasts (ECMWF) or performed well compared with standard numerical weather prediction [38]. Thus, we can expect the accuracy of weather forecast will keep improving. Although the prediction of rainfall was out of expectation, the proposed scheme performed better in production and net income compared with other irrigation methods.

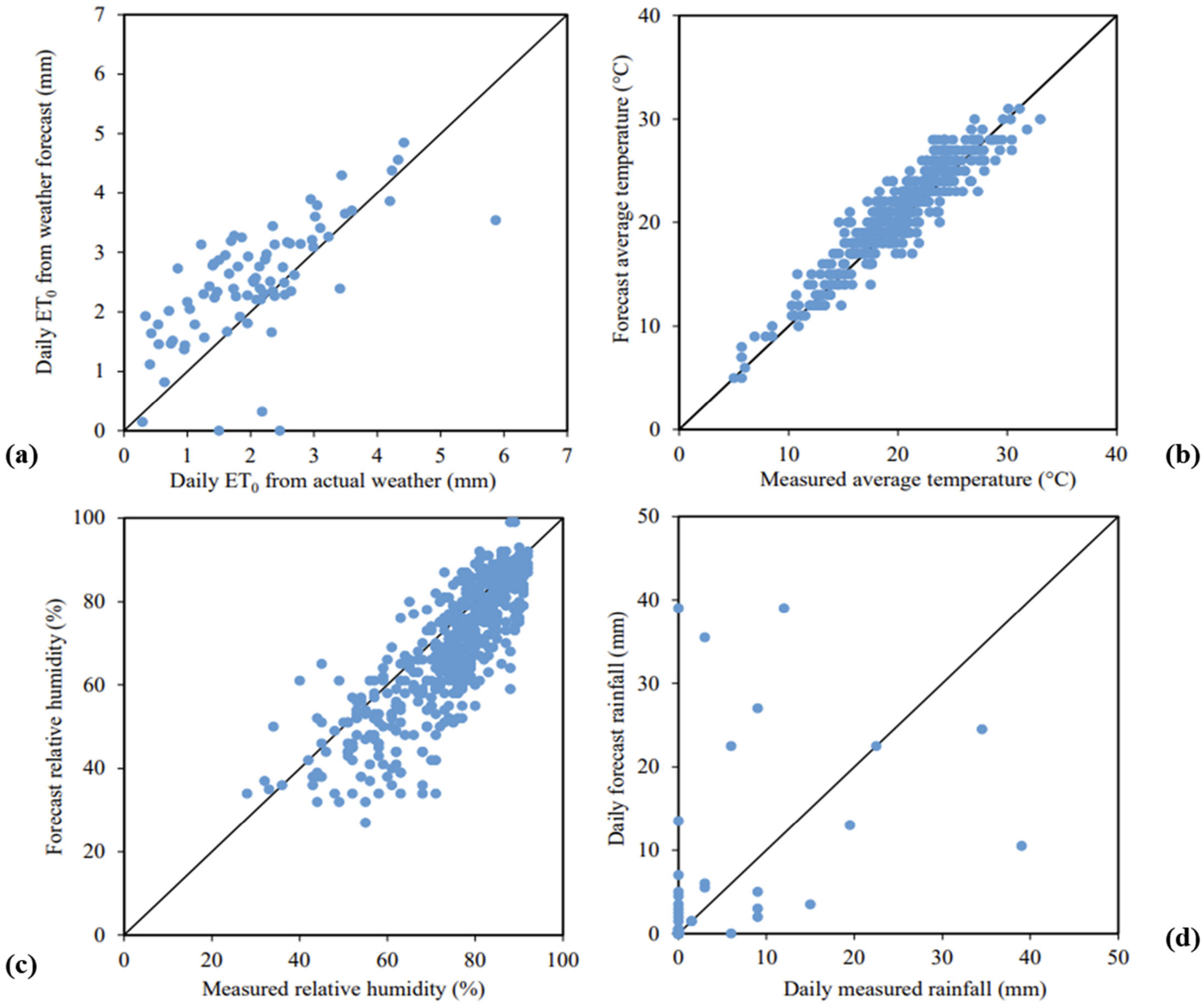

Figure 16. The comparison between weather station measured and forecast weather factors. (**a**) reference evapotranspiration (ET_0), mm; (**b**) hourly average temperature, °C; (**c**) hourly relative humidity, %; (**d**) daily rainfall, mm.

4. Conclusions

A newly proposed irrigation scheme incorporating WF and targeting with maximum net income by running a numerical model, WASH_2D, was applied to potato cultivation on a sandy soil for two seasons, which could save one third time compared with original scheme proposed by Fujimaki et al. [21]. In this study, net income using proposed irrigation scheme was compared with an automated and refilling irrigation scheme in two seasons. During the first season (from April to July), treatment S1 obtained 19% higher net income and 19% larger yield, and saved the water by 28% compared with A. Meanwhile, compared with A, the nitrogen uptake of S1 was improved by 39%. In the second season (from August to December), due to low temperature and solar radiation at late growth stage, the total irrigation amounts of S2 and R were halved of those in the first season, which lead to lower yield. Although the yield and net income of two treatments in the second season has no significant difference, S2 improved nitrogen uptake by 11% compared with R, which suggests that the scheme may contribute for reducing fertilizer input. As for the accuracy of model, the simulated values of water content were in fair agreement with those measured in the root zone. As for the accuracy of weather forecast, although there was somewhat large deviation between the predicted rainfall and measured one, the derived comprehensive weather factor, ET_0, were within acceptable error range. Contribution of rainfall in drylands to total water supply is far lower than that in the place where this study was carried out. On the other hand, as explained in the text, the higher nitrate leaching of the proposed irrigation scheme compared with other two irrigation schemes under the current sandy soil and climate condition should also be noted. Considering the improved NU_PE and net income, reducing fertilizer inputs would be one of the options to eliminate the nitrate leaching issue in sandy soil, which has low water and nutrient holding capacity and high soil drainage. More studies on reconciling environmental pollution and farmer's income will be conducted in future.

In general, this study revealed that the proposed irrigation scheme combined with weather forecast could reduce water use and improved yield and net income compared with automatic irrigation in sandy soil, which could largely benefit for farmers. Though the proposed scheme has less advantage when compared with refilling irrigation, the enhanced nitrogen uptake efficiency should also be taken into consideration. This study would present an irrigation scheme that could improve net income of farmers and has potential to decrease fertilizer input in future.

Author Contributions: S.L. conceived and designed the study; Collected data and performed the analysis; Wrote the paper. H.M.A.E.B. conceived and designed the study; Contributed to data analysis. P.A. contributed to editing to the draft of the manuscript, and supervision of the study. H.F. conceived, designed and supervised of the study, and provided a critical review and editing to the manuscript. All authors contributed to revision, read and approval of the submitted version of this manuscript. All authors have read and agreed to the published version of the manuscript.

Funding: This research received no external funding.

Institutional Review Board Statement: Not applicable.

Informed Consent Statement: Not applicable.

Data Availability Statement: The data presented in this study are available on request from the corresponding author. WASH_2D model and necessary parameters can be download from the following link: http://www.alrc.tottori-u.ac.jp/fujimaki/download/WASH_2D/, accessed on 26 September 2022.

Acknowledgments: This work was financially supported by The United Graduated School of Agricultural Sciences, Tottori University. We thank the university for providing generous funding. We appreciate the collaboration and assistance of the staff of the Arid Land Research Center of Tottori university.

Conflicts of Interest: The authors declare that they have no known competing financial interests or personal relationships that could have appeared to influence the work reported in this paper.

References

1. Fereres, E.; Soriano, M.A. Deficit irrigation for reducing agricultural water use. *J. Exp. Bot.* **2007**, *58*, 147–159. [CrossRef] [PubMed]
2. Ward, F.A.; Pulido-Velazquez, M. Water conservation in irrigation can increase water use. *Proc. Natl. Acad. Sci. USA* **2008**, *105*, 18215–18220. [CrossRef] [PubMed]
3. Wada, Y.; Bierkens, M.F.P. Sustainability of global water use: Past reconstruction and future projections. *Environ. Res. Lett.* **2014**, *9*, 104003. [CrossRef]
4. Liu, J.; Hertel, T.W.; Lammers, R.B.; Prusevich, A.; Baldos, U.L.C.; Grogan, D.S.; Frolking, S. Achieving sustainable irrigation water withdrawals: Global impacts on food security and land use. *Environ. Res. Lett.* **2017**, *12*, 104009. [CrossRef]
5. Geerts, S.; Raes, D. Deficit irrigation as an on-farm strategy to maximize crop water productivity in dry areas. *Agric. Water Manag.* **2009**, *96*, 1275–1284. [CrossRef]
6. Volschenk, T. Water use and irrigation management of pomegranate trees—A review. *Agric. Water Manag.* **2020**, *241*, 106375. [CrossRef]
7. Singh, B.R.; Singh, D.P. Agronomic and physiological-responses of sorghum, maize and pearl-millet to irrigation. *Field Crop. Res.* **1995**, *42*, 57–67. [CrossRef]
8. Cabello, M.J.; Castellanos, M.T.; Romojaro, F.; Martinez-Madrid, C.; Ribas, F. Yield and quality of melon grown under different irrigation and nitrogen rates. *Agric. Water Manag.* **2009**, *96*, 866–874. [CrossRef]
9. Cai, X.M.; Hejazi, M.I.; Wang, D. Value of Probabilistic Weather Forecasts: Assessment by Real-Time Optimization of Irrigation Scheduling. *J. Water Resour. Plan. Manag.* **2011**, *137*, 391–403. [CrossRef]
10. Cao, J.J.; Tan, J.W.; Cui, Y.L.; Luo, Y.F. Irrigation scheduling of paddy rice using short-term weather forecast data. *Agric. Water Manag.* **2019**, *213*, 714–723. [CrossRef]
11. Linker, R.; Sylaios, G. Efficient model-based sub-optimal irrigation scheduling using imperfect weather forecasts. *Comput. Electron. Agric.* **2016**, *130*, 118–127. [CrossRef]
12. Brown, D.J. Using a global VNIR soil-spectral library for local soil characterization and landscape modeling in a 2nd-order Uganda watershed. *Geoderma* **2007**, *140*, 444–453. [CrossRef]
13. Lorite, I.J.; Ramirez-Cuesta, J.M.; Cruz-Blanco, M.; Santos, C. Using weather forecast data for irrigation scheduling under semi-arid conditions. *Irrig. Sci.* **2015**, *33*, 411–427. [CrossRef]
14. Muller, C.F.; Neal, M.B.; Carey-Smith, T.K.; Luttrell, J.; Srinivasan, M.S. Incorporating weather forecasts into risk-based irrigation decision-making. *Australas. J. Water Resour.* **2021**, *25*, 159–172. [CrossRef]
15. Anupoju, V.; Kambhammettu, B.P.; Regonda, S.K. Role of Short-Term Weather Forecast Horizon in Irrigation Scheduling and Crop Water Productivity of Rice. *J. Water Resour. Plan. Manag.* **2021**, *147*, 5021009. [CrossRef]
16. Simionesei, L.; Ramos, T.B.; Palma, J.; Oliveira, A.R.; Neves, R. IrrigaSys: A web-based irrigation decision support system based on open source data and technology. *Comput. Electron. Agric.* **2020**, *178*, 105822. [CrossRef]
17. Ajdary, K.; Abianeh, H.Z. Modeling of nitrogen leaching by using urea fertilizer in sandy loam soil. *Microorg. Ind. Environ.* **2011**, 71–75. [CrossRef]
18. Wang, Z.; Li, J.S.; Li, Y.F. Simulation of nitrate leaching under varying drip system uniformities and precipitation patterns during the growing season of maize in the North China Plain. *Agric. Water Manag.* **2014**, *142*, 19–28. [CrossRef]
19. Eltarabily, M.G.; Bali, K.M.; Negm, A.M.; Yoshimura, C. Evaluation of Root Water Uptake and Urea Fertigation Distribution under Subsurface Drip Irrigation. *Water* **2019**, *11*, 1487. [CrossRef]
20. Liao, R.K.; Zhang, S.R.; Zhang, X.; Wang, M.F.; Wu, H.R.; Zhangzhong, L.L. Development of smart irrigation systems based on real-time soil moisture data in a greenhouse: Proof of concept. *Agric. Water Manag.* **2021**, *245*, 106632. [CrossRef]
21. Fujimaki, H.; Tokumoto, I.; Saito, T.; Inoue, M.; Shibata, M.; Okazaki, T.; El Mokh, F. *Practical Applications of Agricultural System Models to Optimize the Use of Limited Water*; American Society of Agronomy: Madison, MI, USA, 2014; pp. 209–235.
22. Baki, H.M.A.; Raoof, M.; Fujimaki, H. Determining Irrigation Depths for Soybean Using a Simulation Model of Water Flow and Plant Growth and Weather Forecasts. *Agronomy* **2020**, *10*, 369. [CrossRef]
23. El Baki, H.M.; Fujimaki, H. An Evaluation of a New Scheme for Determination of Irrigation Depths in the Egyptian Nile Delta. *Water* **2021**, *13*, 2181. [CrossRef]
24. Feddes, R.A.; Raats, P.A.C. Parameterizing the soil-water-plant root system. In *Unsaturated-Zone Model*; Progress, Challenges Applications; Kluwer Academic Publishers: Dordrecht, The Netherlands, 2004.
25. Van Genuchten, M.T. *A Numerical Model for Water and Solute Movement in and below the Root Zone*; United States Department of Agriculture Agricultural Research Service US Salinity Laboratory: Riverside, CA, USA, 1987.
26. Allen, R.G.; Pereira, L.S.; Raes, D.; Smith, M. *Crop Evapotranspiration. Guidelines for Computing Crop Water Requirements*; FAO Irrigation and Drainage Paper (FAO): Rome, Italy, 1998.
27. Abd El Baki, H.M.; Fujimaki, H.; Tokumoto, I.; Saito, T. A new scheme to optimize irrigation depth using a numerical model of crop response to irrigation and quantitative weather forecasts. *Comput. Electron. Agric.* **2018**, *150*, 387–393. [CrossRef]
28. Feddes, R.A.; Zaradny, H. Model for simulating soil-water content considering evapotranspiration—Comments. *J. Hydrol.* **1978**, *37*, 393–397. [CrossRef]
29. Fujimaki, H.; Ando, Y.; Cui, Y.B.; Inoue, M. Parameter estimation of a root water uptake model under salinity stress. *Vadose Zone J.* **2008**, *7*, 31–38. [CrossRef]

30. Cornish, G.; Bosworth, B.; Perry, C.; Burke, J. *Water Charging in Irrigated Agriculture: An Analysis of International Experience*; Food & Agriculture Organization: Rome, Italy, 2004; p. 28.
31. Martínez-Romero, A.; Domínguez, A.; Landeras, G. Regulated deficit irrigation strategies for different potato cultivars under continental Mediterranean-Atlantic conditions. *Agric. Water Manag.* **2019**, *216*, 164–176. [CrossRef]
32. Williams, M.M.; Masiunas, J.B. Functional relationships between giant ragweed (Ambrosia trifida) interference and sweet corn yield and ear traits. *Weed Sci.* **2006**, *54*, 948–953. [CrossRef]
33. Kross, A.; McNairn, H.; Lapen, D.; Sunohara, M.; Champagne, C. Assessment of RapidEye vegetation indices for estimation of leaf area index and biomass in corn and soybean crops. *Int. J. Appl. Earth Obs. Geoinf.* **2015**, *34*, 235–248. [CrossRef]
34. Weraduwagel, S.M.; Chen, J.; Anozie, F.C.; Morales, A.; Weise, S.E.; Sharkey, T.D. The relationship between leaf area growth and biomass accumulation in *Arabidopsis thaliana*. *Front. Plant Sci.* **2015**, *6*, 167. [CrossRef]
35. Gao, Y.; Xu, Z.; Zhang, L.; Li, S.; Wang, S.; Yang, H.; Liu, X.; Zeng, D.; Liu, Q.; Qian, Q.; et al. MYB61 is regulated by GRF4 and promotes nitrogen utilization and biomass production in rice. *Nat. Commun.* **2020**, *11*, 5219. [CrossRef]
36. Huang, T.; Ju, X.; Yang, H. Nitrate leaching in a winter wheat-summer maize rotation on a calcareous soil as affected by nitrogen and straw management. *Sci. Rep.* **2017**, *7*, 42247. [CrossRef] [PubMed]
37. Hoogenboom, G. Contribution of agrometeorology to the simulation of crop production and its applications. *Agric. For. Meteorol.* **2000**, *103*, 137–157. [CrossRef]
38. Frnda, J.; Durica, M.; Rozhon, J.; Vojtekova, M.; Nedoma, J.; Martinek, R. ECMWF short-660 term prediction accuracy improvement by deep learning. *Sci. Rep.* **2022**, *12*, 7898. [CrossRef] [PubMed]